Published in final edited form as:
Razi, H., Predan, J., Fischer, F. D., Kolednik, O., & Fratzl, P. (2020). Damage tolerance of lamellar bone. Bone, 130: 115102. doi:10.1016/j.bone.2019.115102.

Damage tolerance of lamellar bone

H. Razi, J. Predan, F. D. Fischer, O. Kolednik, P. Fratzl

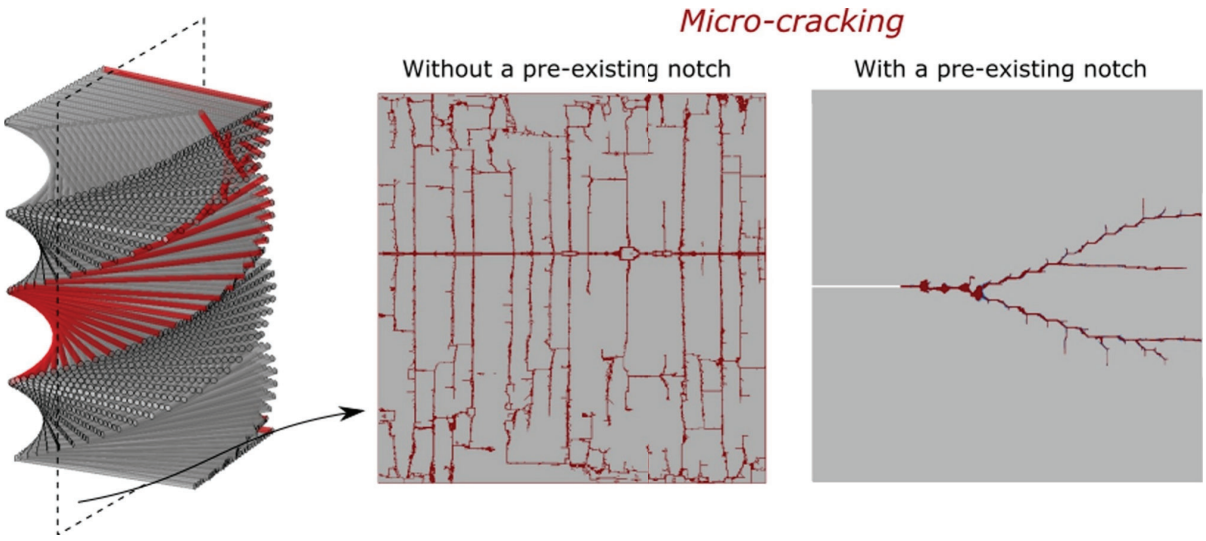

Damage tolerance of lamellar bone

Hajar Razi[1], Jozef Predan[2], Franz Dieter Fischer[3], Otmar Kolednik[4], Peter Fratzl[1,*]

[1]Max Planck Institute of Colloids and Interfaces, Department of Biomaterials, Research Campus Golm, 14424 Potsdam, Germany
[2]Faculty of Mechanical Engineering, University of Maribor, SI-2000 Maribor, Slovenia
[3]Institute of Mechanics, Montanuniversitaet Leoben, Franz-Josef Strasse 18, A-8700 Leoben, Austria
[4]Erich Schmid Institute of Materials Science, Austrian Academy of Sciences, Jahnstrasse 12, A-8700 Leoben, Austria

* Corresponding author; mail address: fratzl@mpikg.mpg.de (P. Fratzl).

Dedicated to the memory of John D. Currey

Abstract

Lamellar bone is known to be the most typical structure of cortical bone in large mammals including humans. This type of tissue provides a good combination of strength and fracture toughness. As has been shown by John D Currey and other researchers, large deformations are associated with the appearance of microdamage that optically whitens the tissue, a process that has been identified as a contribution to bone toughness. Using finite-element modelling, we study crack propagation in a material with periodic variation of mechanical parameters, such as elastic modulus and strength, chosen to represent lamellar bone. We show that a multitude of microcracks appears in the region ahead of the initial crack tip, thus dissipating energy even without a progression of the initial crack tip. Strength and toughness are shown to be both larger for the (notched) lamellar material than for a homogeneous material with the same average properties and the same initial notch. The length of the microcracks typically corresponds to the width of a lamella, that is, to several microns. This simultaneous improvement of strength and toughness may explain the ubiquity of lamellar plywood structures not just in bone but also in plants and in chitin-based cuticles of insects and arthropods.

Highlights:

- Finite element models predicted Crack and damage propagation in a lamellar material
- Microcracks ahead of the crack tip dissipate energy without crack progression
- Strength and toughness are larger for the lamellar material than for a homogeneous
- The shortest microcracks extend over one to several lamellae (few microns)
- The advantage of the inhomogeneity is greatest for intrinsically brittle materials

Introduction

"When bone starts to break thousands of little microcracks form. These microcracks are positioned sensibly in relation to the histological structure of the bone, but we don't know where they form in relation to the ultrastructure. Typically when microcracks form they only reach a few microns in length before they come to a halt. The big question is, what brings them to a halt?" (John D. Currey in [1]).

The mechanical properties of cortical bone represent an ideal compromise between sufficient strength and remarkable toughness [2]. This is achieved by a hierarchical organisation of the bone tissue [3, 4], whereby interfaces between building blocks at many length scales reduce the fragility of mineralized tissue [5, 6]. In addition to its obvious mechanical function, human cortical bone is pervaded by a hierarchical network of pores, corresponding to canals with tens of microns, cell lacunae with microns and canaliculi with hundreds of nanometer diameter, which are all needed for the bone's function as endocrine organ involved in the homeostasis of both calcium and phosphate ions [7, 8]. These pores interrupt the continuity of the material consequently it has been discussed whether they might act as stress concentrators weakening the material [9, 10]. Nevertheless, cortical bone behaves mechanically remarkably well despite this multitude of "defects" in the structure. This tolerance against defects or damage may also be related to a relatively low "*notch sensitivity"* of bone [11], whereby a perfectly notch-insensitive material would show a decrease in strength equal only to the reduction in cross-sectional area, while a notch-sensitive material would show a disproportionately larger reduction [12].

To a large extent, bone stiffness is related to the mineral content of the tissue [13-20]. For instance, the middle ear ossicles are favourably stiff owing to their high amounts of mineralization [21]. Bone structure, anisotropy, and particularly porosity have also proven important for bone stiffness [20]. But mineral content is less predictive of tensile strength, despite its relation to the Young's modulus [14]. Strength as well as toughness, as the ability of material to resist fracture and hinder crack propagation, are essential properties of cortical bone which are less understood. In particular, when bone is imposed to absorb more energy than elastically possible, it is important to understand how it dissipates this energy [22]. Many aspects of bone toughness have been previously discussed [2, 23].

One interesting aspect is that microcracking occurs in bone undergoing large strains (Fig. 1), which is believed to allow bone to absorb a substantial amount of energy before fracture [24, 25]. It has been argued that microcracking is an important prerequisite of a bone being tough [26]. Reilly and Currey showed a progressive increase in tensile microcracking in bone specimens as strain increases. Eventually the microcracks coalesce to form fatal macro cracks only at high strains when the microcracking becomes very dense [27]. Reilly and Currey also showed the failure crack to be highly convoluted with very dense tensile microcracks around them and to be spatially associated with higher mineralized regions of bone [28]. Furthermore, they observed flame-like arrays of microdamage [26, 28], similar to the focal areas of diffuse straining reported by Burr et al. [29] and the network of cracks described by Boyce et al. [30]. Other authors followed up cracks in more details using light scattering induced by microcracks, leading to an apparent whitening of the material in the process zone

(a feature similar to stress-whitening due to crazing in polymers) where non-linear mechanisms arise [31]. The developed *whitening* was shown to be associated with extensive micro-cracking and diffuse damage formation ahead of the crack tip preventing the macro-crack formation [31]. Several authors believe that microcracking is less advantageous [32] and weakens bone leading to stress concentrations and catastrophic failure [33-35]. In a more general context, micro-crack toughening is common in certain engineering ceramic composites. The main effect is that the formation of micro-cracks leads to a reduction of the crack driving force for the macro crack due to decrease of the stiffness (or apparent elastic modulus) in the process zone. Moreover, the formation and growth of micro-cracks also enhance the energy dissipation during fracture [36]. This decrease in crack driving force leads to toughening of the material, since a higher load is required for propagating the macro-crack. Nevertheless, a better theoretical understanding of cause and effect relationships between microcracking and toughness seems essential.

Most bone tissues exist in two distinct forms: woven and lamellar. Woven bone is laid rapidly and considered to have inferior material properties compared with the lamellar bone [6], though little evidence of its mechanical property exists. It consists of generally more mineralized [37] randomly-oriented thin collagen fibers [3]. Lamellar bone consists of fine lamellae put down much more slowly than woven bone. Layers of parallel collagen fibrils are deposited with an orientation that changes along an axis perpendicular to the lamellae, sometimes with thin sublayers of unordered collagen (Fig. 2A) [38]. Since mechanical properties are strongly anisotropic in mineralized collagen fibrils [39], they will vary along this axis in lamellar bone, essentially leading to a material with periodically varying modulus and strength [40].

For a crack to grow in a material, its crack driving force should exceed the crack growth resistance. The crack driving force originates from the work of the applied forces and depends essentially on the elastic properties of the material, while the crack growth resistance is an intrinsic material property [41]. Recent analytical calculations and numerical simulations show that the crack driving force is strongly reduced in a material with periodically varying elastic modulus, such as lamellar bone [40, 42, 43]. Given the fact that the crack driving force depends on elastic properties, its reduction in layered materials is independent of the fact whether they are inherently tough or brittle. However, the crack growth resistance in a layered material is more difficult to assess, at least with analytical theories.

In this work, we use finite element simulation of a simple model for a layered material to study the effect of layering on crack propagation in terms of progressive damage evolution and failure. The periodic material is set up so as to represent the known characteristics of lamellar bone for modulus and strength [39], with different assumptions about damage energies. Pre-existing cracks of different lengths are considered, since the presence of cracks is expected to reduce the (nominal) strength of the material as compared to a perfect defect free material, essentially according to the Griffith rule [44]. The goal of this study was to test the hypothesis that lamellar bone structure not only contributes to toughness by energy dissipation through microcracking, but that it also reduces the material's sensitivity to cracks and other defects. Ultimately, we wanted to give a tentative answer to John Currey's question in the quote cited at the beginning of the Introduction.

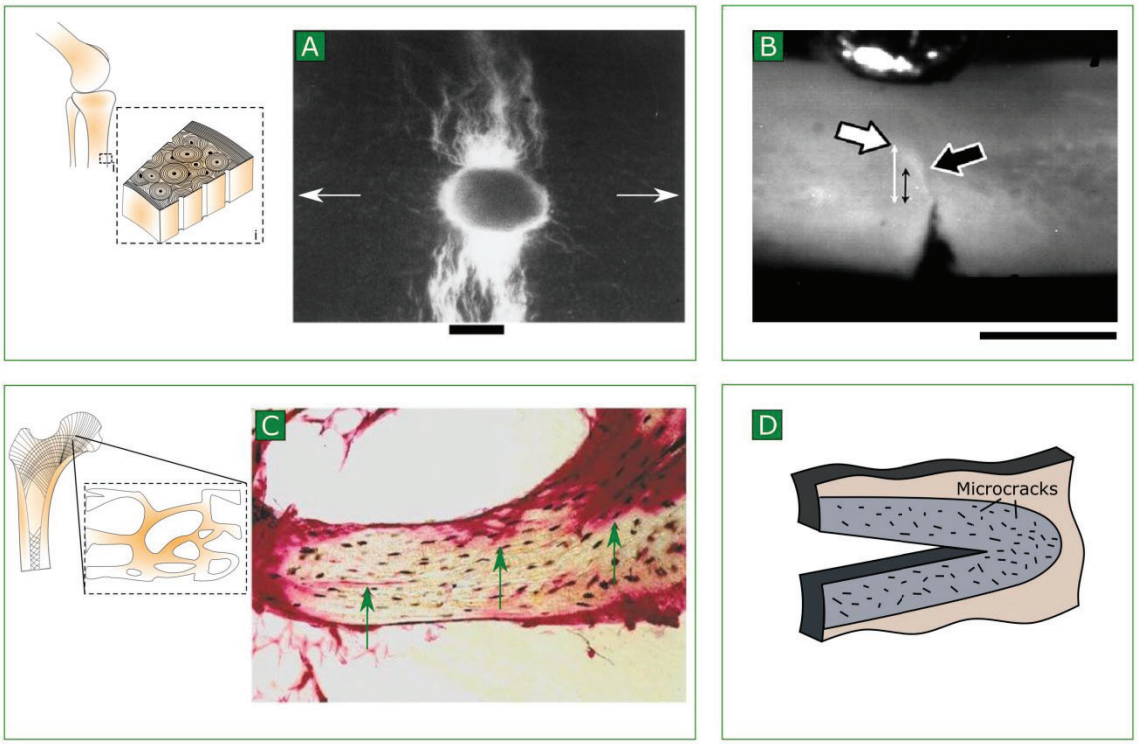

Figure 1. Microcracking in bone. (A) A specimen of bovine tibia loaded in four point bending (loading direction is shown by arrows). Brightly stained diffuse microcracks can be seen at the top and bottom of the blood vessel, i.e. the dark hole in the center. Scale bar = 50 μm; reprinted from [28] with permission from Elsevier. (B) Gamma corrected frames of a rat tibia sample showing the crack tip (black arrow) and the whitening front (white arrow) propagation during three points bending. Double arrowed lines represent the distance of the crack tip and the whitening front from the pre-notch; reprinted from [31] with permission. (C) Microdamage in cancellous bone revealed by staining with basic fuchsin (pink). The arrows indicate (from left to right): a microcrack, cross-hatching and diffuse damage, respectively; reprinted from [45] with permission from Elsevier. (D) Extrinsic toughening of bone tissue by constrained microcracking; reprinted from [2] with permission.

Methods

We study the fracture behavior in human lamellar bone using a 2D finite element model for predicting progressive damage evolution and failure in tensile specimens with and without pre-existing notches (i.e. initial crack). We use a phenomenological model known as "ductile damage plasticity model", which uses as criterion for damage initiation the situation when the incremental equivalent plastic strain ($\bar{\varepsilon}_D^{pl}$) meets the condition $\int(d\bar{\varepsilon}^{pl}/\bar{\varepsilon}_D^{pl})$=1. The model assumes that a critical equivalent plastic strain $\bar{\varepsilon}_D^{pl}$ is required to initiate damage in an individual layer, so that damage evolution is controlled by specific damage evolution energy. Increasing damage is linked to linearly decreasing stiffness and strength, i.e. both the elastic modulus and the strength of the damaged elements decrease to zero during damage evolution from 0 to 1. Lamellar bone is modelled as a continuous but periodically inhomogeneous material consisting of layers with varying mechanical properties, chosen to correspond to lamellar bone with a given fiber orientation (λ = 5 μm, where λ denotes the distance between sublayers with fiber angles 0˚ and 180˚).

As input for the model, we deduce the conventional elastic and plastic material properties from previous experimental data [23, 39], whereby the variations of Young's modulus and strength are calculated from the anisotropy of the composite and the rotated position of fibers along the axis perpendicular to the layers (Fig. 2B-C) [40]. Such a model for lamellar bone is compared to one with constant average material properties, homogeneous throughout the specimen. We compare the nominal strength and the energy to failure for models with different values of damage evolution energy. The inherent specific damage evolution energy in the material is, however, not known from experiment. To explore its influence, we study two versions of the model, one with a low damage evolution energy (Γ_{DE} = 0.001 J/m^2; describing a material that is inherently more brittle) and one with a larger value of this energy (Γ_{DE} = 1 J/m^2).

Table 1 lists the individual parameters (E: Young's modulus, σ_y: Strength, $\varepsilon_{Pl,DI}$: plastic strain at damage initiation) included in the inhomogeneous material for each confined layer in the model, i.e. 200 nm-thick sublayers, each with a given collagen fiber orientation, θ. In addition, properties of the average homogeneous material are given for comparison. An isotropic constant Poisson's ratio of 0.3 is assumed throughout all the models. Minimal strain hardening is considered in both homogeneous and inhomogeneous models: The increase in strength between yield point and damage initiation is assumed to be $\Delta\sigma = 1$ MPa, which is small compared to the yield stress (see Table 1). Density has been considered globally constant in all the models (1000 kg/m^3).

Table 1

Model	θ (˚)	E (GPa)	σ_y *(MPa)*	$\varepsilon_{\mathrm{Pl,DI}}$ (1/1)
Average homogeneous	-	1.52	16.1	0.0079
Periodic inhomogeneous material	0	7.83	75.9	0.0050
	7.5	5.37	48.1	0.0050
	15	2.82	28.1	0.0050
	22.5	1.64	18.8	0.0050
	30	1.08	13.8	0.0050
	37.5	0.80	10.7	0.0051
	45	0.63	8.7	0.0053
	52.5	0.54	7.3	0.0063
	60	0.48	6.4	0.0080
	67.5	0.44	5.7	0.0102
	75	0.42	5.3	0.0123
	82.5	0.41	5.0	0.0140
	90	0.40	4.9	0.0149

Numerical analyses are performed with a commercial implementation of the finite element program Abaqus (Dassault Systèmes, Johnston, RI). In order to avoid numerical instabilities after onset of the damage evolution, direct-integration dynamic analyses (for quasi static application) are used. Models are 2D squares of 100-by-100 μm^2 (with 0.1 μm nominal thickness; note that the magnitude of the nominal thickness does not have any effect on the computational results). Each model consists of 2.5E+5 4-noded plane stress elements of 0.2-by-0.2 μm^2 in size. We look at models with and without pre-existing cracks. Pre-existing

cracks are located in the middle of the left boundaries inserted by removing a single row of elements in the models. The crack length, a, varies from 0.2 to 50 μm, i.e. 0.2% to 50% of the model width (W). A small disturbance (by removing a single element in the middle of the specimen) was inserted into the models with a/W = 0.002 in order to avoid numerical artefacts [46]. Models are subjected to a prescribed displacement at the top boundary u_y. The lower boundary nodes were restricted in y-direction, i.e. loading direction. A single node at the lower left corner of the specimen was restricted to move in x-direction, i.e. perpendicular to load direction.

Results are visualized in terms of crack and damage propagation, i.e. the elements with 100% stiffness degradation and softening after damage initiation were removed from the model (see Fig. 3A, regions underwent damage and cracking are shown in blue and red, respectively). Global reaction force versus displacement curves are extracted from the models and used to deduce the nominal strength ($\sum RF \,/\, Area$) and energy to fracture (i.e. area under the force-displacement curve).

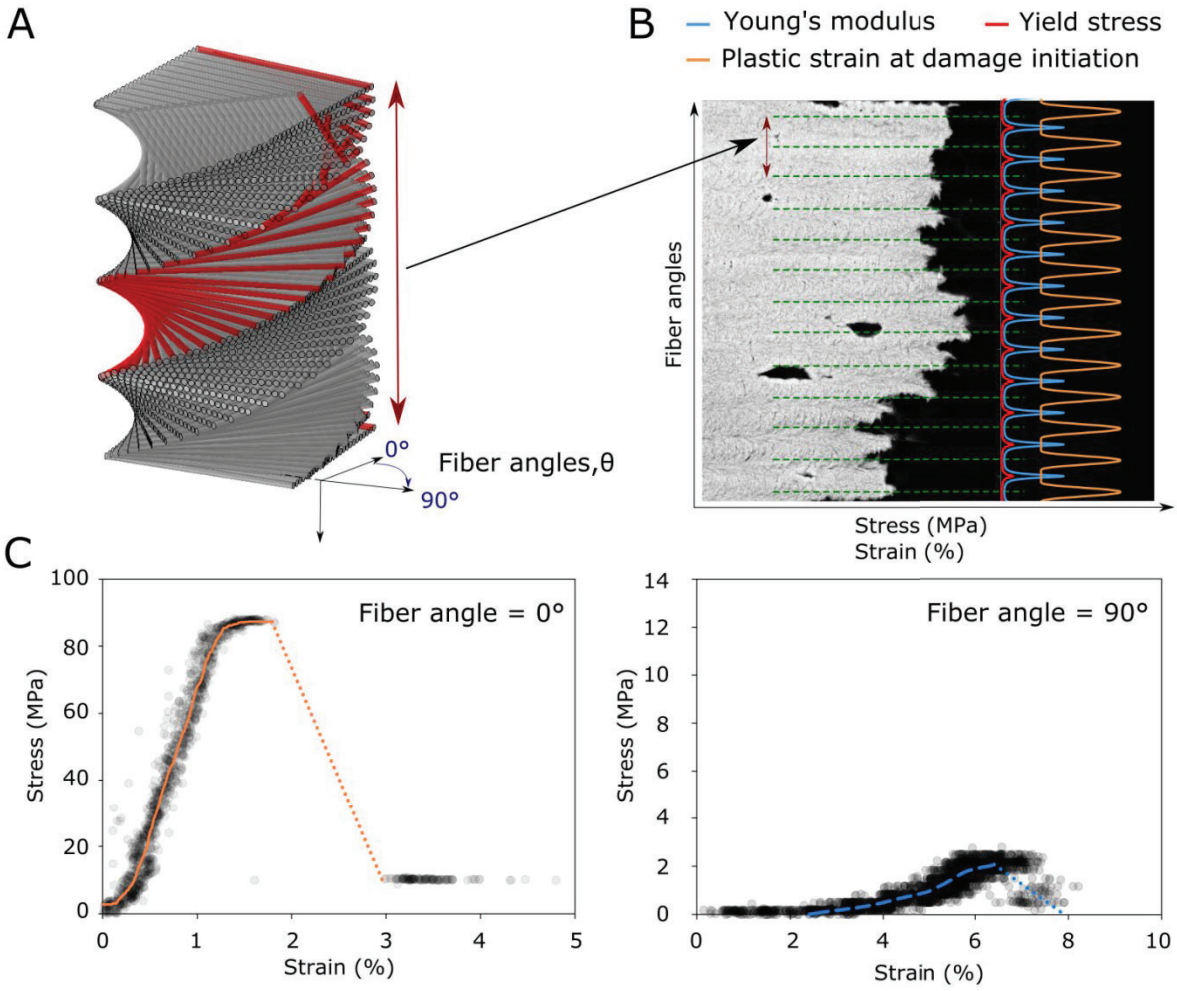

Figure 2. (A) Schematic drawing of plywood arrangement of collagen fibrils in bone. Fiber rotation angles θ vary from 0˚ to 90˚, i.e. from perpendicular to parallel to the cross-section, respectively. The drawing represents two bone lamellae as shown in panel (B). (B) Variation of mechanical properties of bone with respect to its fiber orientations as can be seen in an SEM image of human lamellar bone

next to a crack front [23]. (C) Stress-strain curves for two most prominent fiber directions in (fully hydrated) fibrolamellar cortical samples of bovine bone [39].

Results and Discussion

A few examples of crack patterns and damage propagation are shown in Fig. 3A for models with homogeneous and periodically inhomogeneous material properties. Damage without fracture (i.e. degraded but not fully fractured material) is shown in blue and (micro-)cracks in red (i.e. 100% degraded material). The typical spacing between vertical lines (that correspond to damage as well as cracks) corresponds to the thickness of one or several lamellae (as defined by the periodicity of the properties in horizontal direction). Accordingly, micro-cracks in the normal (horizontal) propagation direction have a typical length of one period, that is, several microns. Fig. 3A shows that we have continuous damage evolution and crack propagation in the homogeneous materials. The behavior of (essentially unnotched, i.e. with single element removed from the model) tensile specimens (a/W = 0.002) depends on the magnitude of the damage evolution energy Γ_{DE}. For very brittle materials (Γ_{DE} low), damage concentrates along a (horizontal) plane with maximum normal stress. For less brittle materials (Γ_{DE} high), damage concentrates along inclined planes with maximum shear stress. This can in principle be observed in homogeneous and inhomogeneous materials. However, damage evolution is discontinuous in the inhomogeneous materials. Crack path is splitting, deformation and damage occur between the layers (blue regions) and microcracks (red in Fig. 3) form that usually span one or several lamellae.

At comparable loading stages, damage appears more widespread in the inhomogeneous materials, which indicates larger energy dissipation than in the homogeneous material. This becomes especially obvious in the case of the more brittle material (lower value of Γ_{DE}). This is also visible in the overall response of the material, as shown in Fig. 3B. which shows the reaction force (RF) plotted against the displacement. It is seen that, with one exception, the RF is higher in the inhomogeneous material compared to the homogeneous material. The exception appears for tensile specimens, i.e. a/W = 0.002, and high Γ_{DE}, where the RFs reach the plastic limit load in both homogeneous and inhomogeneous materials. The critical displacement at failure is always larger in the inhomogeneous material compared to the homogeneous material. Both the area under the curve and the maximum stress are generally higher for the periodically inhomogeneous than for the homogeneous model. This is indicative of higher energy dissipation (toughness) and a larger nominal strength for the inhomogeneous models. The material is generally weaker for longer cracks and when the intrinsic material is more brittle (lower Γ_{DE}).

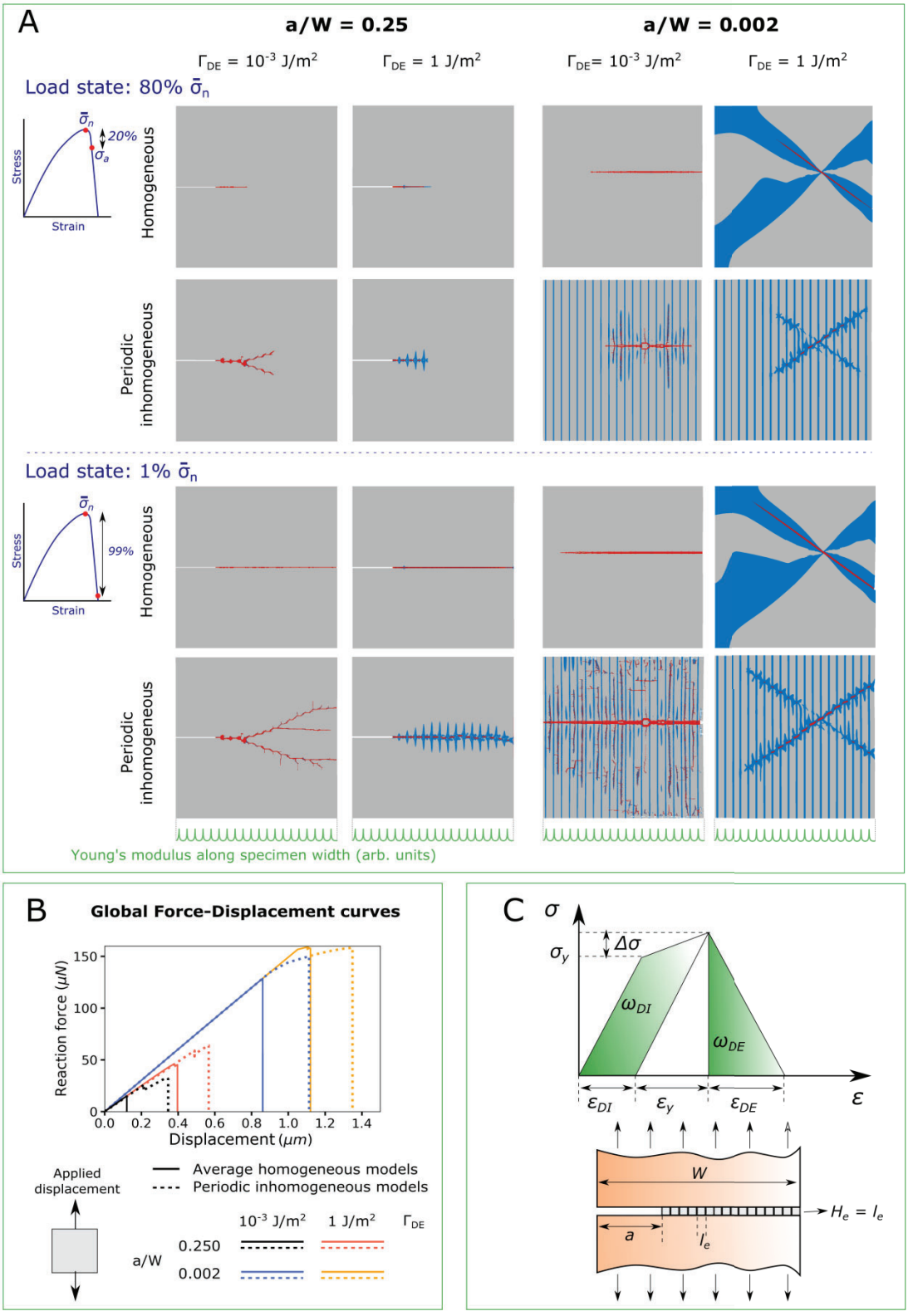

Figure 3. (A) Crack and damage propagation are shown (in red and blue, respectively) for homogeneous average models (top row) vs. periodic inhomogeneous models (bottom row) for tensile specimens with two pre-existing crack lengths a (given in units of specimen width W) and two values of Γ_{DE}. A video showing damage evolution is given in the supplementary material (B) Reaction force vs. prescribed displacement. Units in plot are μN and μm. (C) Top: Parameters included in the ductile damage plasticity model as applied in the current numerical study. Bottom: Pre-existing cracks in the model were determined by removing a row of elements at the middle of left boundary.

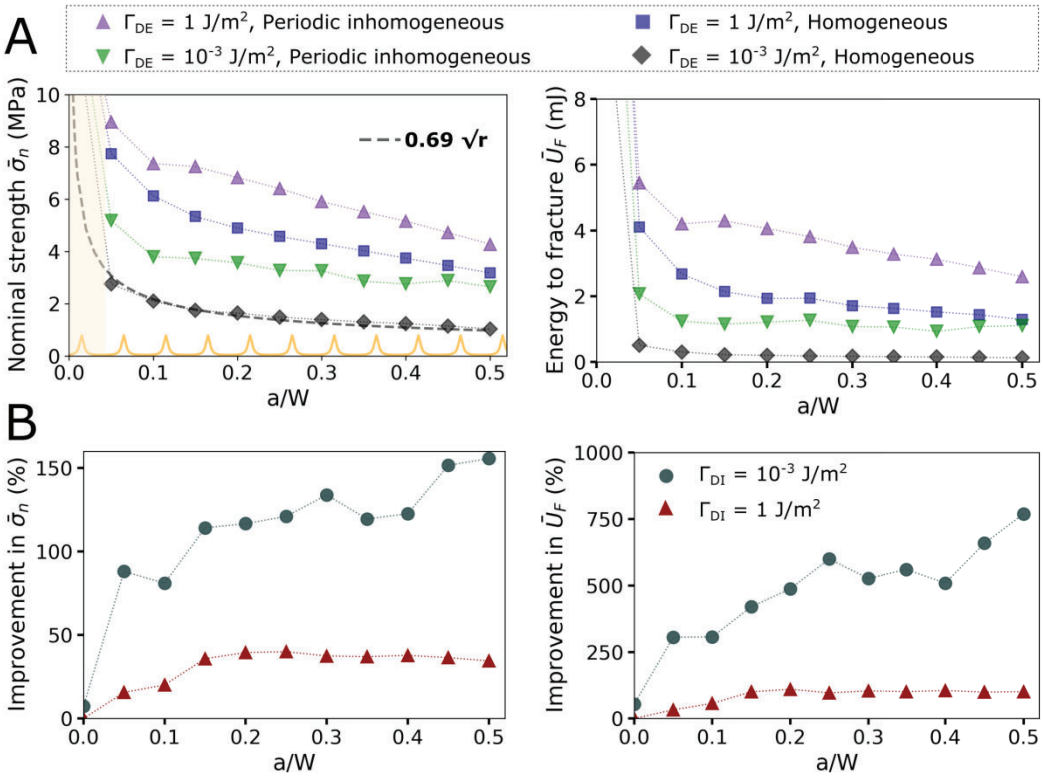

Figure 4. (A) Nominal strength $\bar{\sigma}_n$ and energy to fracture $\bar{U}_F$ of periodic and average homogeneous materials with different level of intrinsic brittleness (Γ_{DE}) as a function of crack length (a/W). Broken line represents a fit to the nominal strength of homogeneous material with Griffith's law [43]. Energy to fracture is calculated as the area under reaction force and displacement curve until total failure. The yellow lines in the bottom of this graph show the variation of Young's modulus in the sample. The period of its variation corresponds to the lamellar thickness. The lower panels (B) show improvements in nominal strength and energy to fracture from the homogeneous to the periodic structure. The length of one period corresponds to a/W = 0.05.

Interestingly, the advantage of the periodic inhomogeneity is more obvious for more brittle materials, when Γ_{DE} is lower. In order to quantify these effects, we looked at the influence of initial crack size on the fracture behavior of both materials in the single edge notched specimen (Fig. 4; in panel A). The nominal strength ($\sum RF_{max}/Area$) is plotted against the initial crack length (a/W). We can see that the homogeneous material behaves close to what we know from Griffith's law, i.e. $\bar{\sigma}_n\sqrt{a}\sim C$. The periodic inhomogeneity results in higher tolerance against initial defects leading to a slower decrease of nominal strength. Fig. 4B shows the improvement in nominal strength and energy to fracture due to the periodic inhomogeneity compared to a homogeneous material with identical average properties. It is obvious that the improvement increases with the initial crack length and when the material is intrinsically more brittle.

Figure 4 reveals a remarkable property of the lamellar material in that both nominal strength and fracture toughness are improved, knowing that these properties are generally in conflict with each other [2]. The reason is not that the layered materials has intrinsically better

properties, but that a large defect (such as crack) deteriorates the intrinsic properties much less when the material is layered. Indeed, the crack driving force due to the stress concentration at the crack tip is strongly reduced when the material is layered [40]. This is likely to improve the nominal strength (Fig. 4C, left). In addition, the inhomogeneity is found here to induce the splitting of the crack and the generation of microcracks which increases the energy dissipated during failure (Fig. 4C, left). It is worth noticing that at extremely low crack lengths a/W (that is, in an essentially defect-free material), there is a much smaller improvement by the layering. This supports the idea that the layering is essentially counteracting the deterioration of the material properties by defects. The same conclusion can be drawn from the fact that the improvement by layering is stronger when the material is more brittle and, therefore, intrinsically more defect-sensitive (red triangles versus blue circles in Fig. 4B).

Of course, these conclusions are based on a comparatively simple model and should be taken with some caution. First, the model is two-dimensional, neglecting possible spiral crack paths that might lead to additional toughening. Moreover, a ductile damage plasticity model was applied in the current numerical study. The material parameters required for the model were determined from published experimental data on parallel fibered bone [39], where modulus and strength are low compared to other (average) values in literature [20]. However, the general behaviour of the model would be similar if all mechanical parameters would be multiplied by a same (arbitrary) factor. Additionally, a difficulty was the unknown magnitude of the specific damage evolution energy Γ_{DE}, as well as its spatial variation as a function of the collagen fibril orientation. In order to investigate the influence of this parameter, we adopted both a very small value, $\Gamma_{DE} = 0.001$ J/m^2, and a value which is reasonable for brittle ceramic type materials, $\Gamma_{DE} = 1$ J/m^2. It should also be mentioned that several numerical issues can appear during modelling. For example, a high magnitude of Γ_{DE} may require a very large strain ε_{DE}, i.e. a very long computation time, if the element size is too small. Moreover, the influences of strain rate and viscoelasticity have not been considered in this study. In fact, it has been shown for fibrolamellar bone that elastic modulus, tensile strength, as well as energy absorption capacity increase at high strain rates [47]. Moreover, the critical equivalent plastic strain for damage initiation implemented in our model might depend on the strain rate. Further studies are needed to explore the likely influence of strain rate on the damage and crack propagation observed in this study especially in the intrinsically more brittle material.

As shown by the schematic stress-strain behavior of a material point (Fig. 3C), a certain plastic strain ε_{DI} is required for damage initiation, which consumes a plastic strain energy of $\omega_{DI} \approx \sigma_y \varepsilon_{DI}$ for damage initiation per unit volume. Note that the increase in stress due to hardening is negligible compared to the yield stress σ_y. The energy dissipated during damage evolution in a unit volume can be written as $\omega_{DE} \approx \frac{1}{2} \sigma_y \varepsilon_{DE}$. The term $\omega_{FR} = \omega_{DE} + \omega_{DI}$ describes the total amount of dissipated energy per unit volume. It is, therefore, important to realize that energy is dissipated both by local plastic deformation and by microcrack formation (damage evolution). It is difficult to disentangle both contributions since they may work synergistically. Indeed, with the formation of microcracks new spots of stress concentration are created, leading to additional plastic deformation, somewhat away from the original crack tip.

Fracture toughness of lamellar bone was previously measured as a function of local collagen fibril orientations in terms of critical J-integral (J_C-) values [23]. Therefore, the question arises whether it is possible to use these measurements for the determination of the magnitude of Γ_{DE} by a numerical simulation of their fracture mechanics experiments and applying the modelling procedure introduced in the current paper. This is, however, an extremely difficult task: The finite element model of the fracture mechanics specimens must have a very fine mesh in order to reflect the periodicity of the mechanical properties of bone, $\lambda = 5$ μm. On the other hand, a fracture mechanics specimen is very large in comparison to λ, e.g. the bend specimen used in [23] had a size of 15×1.5×2 mm^3. Razor blade cutting for introducing an initial crack into a fracture mechanics specimen results in a notch width of approximately 0.1 mm. This means that the notch width has the magnitude of the whole finite element models presented in the current paper.

Conclusions

Finite element calculations using a simple two-dimensional model for a material with periodically varying mechanical properties show the appearance of microcracks ahead of the crack tip. Compared to a homogeneous material with the same average properties, this leads to enhanced energy dissipation and, thus, a higher toughness. Large defects in the material also reduce the nominal strength by a lesser amount than in the homogeneous material. The reason for this higher nominal strength is the reduction of crack driving force already analyzed in previous works [40, 42, 43]. As a consequence, our analysis suggests that both nominal strength and toughness are improved by the periodic modulation of mechanical properties achieved through the lamellar structure in bone. Finally, the typical length of microcracks should correspond to the thickness of individual lamellae in the lamellar bone structure. It also appears in the model that these microcracks could be connected through damage zones that follow the softer regions of the lamellae but do not correspond to cracks (defined by a separation of the surfaces). Hence, lamellar, plywood-like structures in bone and other biological tissues support a strategy where damage tolerance is achieved through imperfection [48], by introducing a variation of material properties as compared to a perfectly homogeneous material.

Acknowledgements

PF is grateful for support by the DFG, in the framework of the Gottfried Wilhelm Leibniz Prize. HR acknowledges the financial support by the Cluster of Excellence at Humboldt University of Berlin “Image Knowledge Gestaltung: An Interdisciplinary Laboratory”. FDF acknowledges support by the Humboldt Foundation through the Humboldt Research Prize. JP, FDF and OK acknowledge support by the Austrian Federal Government and the Styrian Provincial Government under the frame of the Austrian COMET Competence Center Programme (K2 Competence Center on ‘‘Integrated Research in Materials, Processing and Product Engineering’’, Strategic Project P1.3-WP2).

References

[1] C. Fleck, In memoriam - John D. Currey, 1932-2018, J Biomech (Quoting from John D. Currey's web site at the University of York (https://www.york.ac.uk/biology/staff/jdc.htm)) (2019) 1-3.
[2] R.O. Ritchie, The conflicts between strength and toughness, Nat Mater 10(11) (2011) 817-822.
[3] S. Weiner, H.D. Wagner, The material bone: Structure mechanical function relations, Annu Rev Mater Sci 28 (1998) 271-298.
[4] P. Fratzl, H.S. Gupta, E.P. Paschalis, P. Roschger, Structure and mechanical quality of the collagen-mineral nano-composite in bone, J Mater Chem 14(14) (2004) 2115-2123.
[5] J.D. Currey, Materials science - Hierarchies in biomineral structures, Science 309(5732) (2005) 253-254.
[6] W. Wagermaier, K. Klaushofer, P. Fratzl, Fragility of Bone Material Controlled by Internal Interfaces, Calcified Tissue Int 97(3) (2015) 201-212.
[7] L.F. Bonewald, The Amazing Osteocyte, J Bone Miner Res 26(2) (2011) 229-238.
[8] R. Weinkamer, P. Kollmannsberger, P. Fratzl, Towards a Connectomic Description of the Osteocyte Lacunocanalicular Network in Bone, Curr Osteoporos Rep 17(4) (2019) 186-194.
[9] J.D. Currey, Stress Concentrations in Bone, Q J Microsc Sci 103(61) (1962) 111-&.
[10] D.P. Nicolella, D.E. Moravits, A.M. Gale, L.F. Bonewald, J. Lankford, Osteocyte lacunae tissue strain in cortical bone, J Biomech 39(9) (2006) 1735-43.
[11] J.D. Currey, K. Brear, P. Zioupos, Notch sensitivity of mammalian mineralized tissues in impact, P Roy Soc B-Biol Sci 271(1538) (2004) 517-522.
[12] M.N.H. Kelly A., Strong solids, Clarendon Press1986.
[13] J.D. Currey, The design of mineralised hard tissues for their mechanical functions, J Exp Biol 202(23) (1999) 3285-3294.
[14] J. Currey, Incompatible mechanical properties in compact bone, J Theor Biol 231(4) (2004) 569-580.
[15] J.D. Currey, K. Brear, P. Zioupos, The effects of ageing and changes in mineral content in degrading the toughness of human femora, J Biomech 29(2) (1996) 257-260.
[16] J.L. Katz, Hard Tissue as a Composite Material .1. Bounds on Elastic Behavior, J Biomech 4(5) (1971) 455-+.
[17] J.L. Katz, Composite material models for cortical bone., American Society of Mechanical Engineers, New York1981.
[18] T.S. Keller, Predicting the Compressive Mechanical-Behavior of Bone, J Biomech 27(9) (1994) 1159-1168.
[19] C.M. Les, S.M. Stover, J.H. Keyak, K.T. Taylor, A.J. Kaneps, Stiff and strong compressive properties are associated with brittle post-yield behavior in equine compact bone material, J Orthopaed Res 20(3) (2002) 607-614.
[20] J.D. Currey, Bone: Structure and Mechanics, Princeton University Press, Princeton2002.
[21] J.D. Currey, Mechanical-Properties of Bone Tissues with Greatly Differing Functions, J Biomech 12(4) (1979) 313-319.
[22] J. Currey, Whole-bone mechanics: 'The best is the enemy of the good', Vet J 177(1) (2008) 1-2.
[23] H. Peterlik, P. Roschger, K. Klaushofer, P. Fratzl, From brittle to ductile fracture of bone, Nat Mater 5(1) (2006) 52-55.
[24] M.B. Schaffler, W.C. Pitchford, K. Choi, J.M. Riddle, Examination of Compact-Bone Microdamage Using Backscattered Electron-Microscopy, Bone 15(5) (1994) 483-488.
[25] R.B. Martin, Fatigue damage, remodeling, and the minimization of skeletal weight, J Theor Biol 220(2) (2003) 271-6.
[26] P. Zioupos, J.D. Currey, The Extent of Microcracking and the Morphology of Microcracks in Damaged Bone, J Mater Sci 29(4) (1994) 978-986.
[27] G.C. Reilly, J.D. Currey, The development of microcracking and failure in bone depends on the loading mode to which it is adapted, J Exp Biol 202(5) (1999) 543-552.
[28] G.C. Reilly, J.D. Currey, The effects of damage and microcracking on the impact strength of bone, J Biomech 33(3) (2000) 337-343.

[29] D.B. Burr, C.H. Turner, P. Naick, M.R. Forwood, W. Ambrosius, M.S. Hasan, R. Pidaparti, Does microdamage accumulation affect the mechanical properties of bone?, J Biomech 31(4) (1998) 337-345.
[30] T.M. Boyce, D.P. Fyhrie, M.C. Glotkowski, E.L. Radin, M.B. Schaffler, Damage type and strain mode associations in human compact bone bending fatigue, J Orthopaed Res 16(3) (1998) 322-329.
[31] O.L. Katsamenis, T. Jenkins, F. Quinci, S. Michopoulou, I. Sinclair, P.J. Thurner, A Novel Videography Method for Generating Crack-Extension Resistance Curves in Small Bone Samples, Plos One 8(2) (2013).
[32] R.O. Ritchie, J.H. Kinney, J.J. Kruzic, R.K. Nalla, A fracture mechanics and mechanistic approach to the failure of cortical bone, Fatigue Fract Eng M 28(4) (2005) 345-371.
[33] T.L. Norman, Z. Wang, Microdamage of human cortical bone: Incidence and morphology in long bones, Bone 20(4) (1997) 375-379.
[34] M.B. Schaffler, K. Choi, C. Milgrom, Aging and matrix microdamage accumulation in human compact bone, Bone 17(6) (1995) 521-525.
[35] M.R. Forwood, D.B. Burr, Y. Takano, D.F. Eastman, P.N. Smith, J.D. Schwardt, Risedronate Treatment Does Not Increase Microdamage in the Canine Femoral-Neck, Bone 16(6) (1995) 643-650.
[36] D.B. Marshall, B.N. Cox, A.G. Evans, The Mechanics of Matrix Cracking in Brittle-Matrix Fiber Composites, Acta Metall Mater 33(11) (1985) 2013-2021.
[37] J.J. Pritchard, Control or Trigger Mechanism Induced by Mechanical Forces Which Causes Responses of Mesenchymal Cells in General and Bone Apposition and Resorption in Particular, Acta Morphol Neer Sc 10(1-2) (1972) 63-+.
[38] N. Reznikov, R. Shahar, S. Weiner, Three-dimensional structure of human lamellar bone: The presence of two different materials and new insights into the hierarchical organization, Bone 59 (2014) 93-104.
[39] J. Seto, H.S. Gupta, P. Zaslansky, H.D. Wagner, P. Fratzl, Tough lessons from bone: Extreme mechanical anisotropy at the mesoscale, Adv Funct Mater 18(13) (2008) 1905-1911.
[40] F.D. Fischer, O. Kolednik, J. Predan, H. Razi, P. Fratzl, Crack driving force in twisted plywood structures, Acta Biomater 55 (2017) 349-359.
[41] O. Kolednik, Second Edition ed., John Wiley & Sons Inc.2012.
[42] P. Fratzl, H.S. Gupta, F.D. Fischer, O. Kolednik, Hindered crack propagation in materials with periodically varying Young's modulus - Lessons from biological materials, Adv Mater 19(18) (2007) 2657-+.
[43] O. Kolednik, J. Predan, F.D. Fischer, P. Fratzl, Bioinspired Design Criteria for Damage-Resistant Materials with Periodically Varying Microstructure, Adv Funct Mater 21(19) (2011) 3634-3641.
[44] A.A. Griffith, The phenomena of rupture and flow in solids, Philosophical Transactions of the Royal Society of London 221 (1921) 582-593.
[45] N.L. Fazzalari, M.R. Forwood, K. Smith, B.A. Manthey, P. Herreen, Assessment of cancellous bone quality in severe osteoarthrosis: Bone mineral density, mechanics, and microdamage, Bone 22(4) (1998) 381-388.
[46] F.D. Fischer, O. Kolednik, G.X. Shan, F.G. Rammerstorfer, A note on calibration of ductile failure damage indicators, Int J Fracture 73(4) (1995) 345-357.
[47] T.M. Wright, W.C. Hayes, Tensile Testing of Bone over a Wide-Range of Strain Rates - Effects of Strain Rate, Microstructure and Density, Med Biol Eng 14(6) (1976) 671-680.
[48] R. Weinkamer, J.W.C. Dunlop, Y. Brechet, P. Fratzl, All but diamonds Biological materials are not forever, Acta Mater 61(3) (2013) 880-889.